

STRUCTURE AND PROPERTIES OF WELDED JOINTS OF HIGH-STRENGTH STEELS MADE BY METAL-CORED WIRE WITH NITROGEN

A. S. Smolentsev,¹ V. E. Veselova,² A. V. Berezovsky,³
E. A. Usoltsev,⁴ and A. V. Shak⁵

UDC 621.791.011

An austenitic metal-cored wire (diameter – 1.6 mm) with additional nitrogen alloying (0.25–0.40 wt.%) was developed for this study. Mechanical tests and metallographic studies of the deposited metal and welded joints made with austenitic metal-cored wire (composition – Cr20Mn5Ni4Mo2.5Cu3N0.3) were conducted. It was found that the values of σ_u and $\sigma_{0.2}$ of the deposited metal obtained by using the developed wire were 20 to 30% higher compared to the utilized electrode materials, while the ductility characteristics were preserved ($\delta = 43\%$). It was shown that the use of metal-cored wire (Cr20Mn5Ni4Mo2.5Cu3N0.3) for welding of high-strength steel 20HGSNM (EN 1.6523) makes it possible to obtain defect-free welded joints with austenitic-ferritic structure, which have 20% higher strength characteristics compared to the analogues.

Keywords: arc welding, high-strength steels, hull structures, special equipment, metal-cored wire, nitrogen, austenite.

Introduction

During mass production of special equipment, heat-treated high-strength alloy steels of martensitic and martensitic-bainitic grades ($\sigma_u = 1,500\text{--}2,350$ MPa) are used for the manufacture of hull structures [1, 2]. In most cases, the utilized steels have a thickness of 10–20 mm and a hardness of 49–54 HRC, while the carbon content does not exceed 0.35 wt.% [3]. The most common is high-strength alloy steel 20HGSNM (EN 1.6523), which is supplied for welding assembly in a heat-strengthened condition. The mechanical properties and chemical composition of steel 20HGSNM are presented in Ref. [4, 5].

Difficulties during welding of high-strength alloy steels are associated with the appearance of cracks in the weld metal (WM) and heat-affected zone (HAZ) that differ in behavior and formation mechanisms, the inability to achieve the strength of the welded joints equal to that of the base metal (BM) without post-weld heat treatment [2, 6–8], and the need to ensure that WM and HAZ can withstand intense dynamic loads (IDL) [5, 6, 8–10], e.g., resulting from the WM collision with a high-speed (~ 740 m/sec) metallic object [5].

The electrode materials (EM) currently used for welding of high-strength alloy steels are based on austenitic chromium-nickel-manganese steel (solid wire Sv-08H20N9G7T) and low-alloy ferritic-pearlitic steel (solid wire Sv-10GSMT), which do not fully meet the increased requirements for welded joints in terms of strength and performance characteristics [8], as well as IDL [6, 11]. It has been found that the damping capacity of steels and

¹ Ural Federal University named after first President of Russia B. N. Yeltsin, Yekaterinburg, Russia; e-mail: A.S.Smolentsev@mail.ru.

² Institute of Engineering Science UB RAS, Yekaterinburg, Russia; e-mail: le-ra@le-ra.ru.

³ Ural Federal University named after first President of Russia B. N. Yeltsin, Yekaterinburg, Russia; e-mail: a.v.berezovskiy@gmail.com.

⁴ Ural Federal University named after first President of Russia B. N. Yeltsin, Yekaterinburg, Russia; e-mail: e.a.usoltcev@urfu.ru.

⁵ Ural Federal University named after first President of Russia B. N. Yeltsin, Yekaterinburg, Russia; e-mail: a.v.shak@urfu.ru.

alloys is affected by their strength and ability to dampen vibrations, as well as dissipate impact energy based on the principle of redistribution of the centered load into the areal load [12]. High-strength ($\sigma_u > 600$ MPa) alloys and steels with high content of damping elements (Ni, Mn, Cu) and high values of logarithmic decrement damping factor (δ) (e.g., $\delta \approx 0.5\text{--}2.0\%$ (steel 17H18N9) or $\delta \approx 4.0\%$ (alloy HN77TUR) at 600°C) provide maximum reduction of the past-penetration effect at a minimal thickness.

A promising direction for improving the strength characteristics of welded joints is the development of metal-cored wires based on high-strength austenitic steels alloyed with nitrogen [13]. The authors of Ref. [14] describe the results of IDL testing of plates made of austenitic nickel-free steel with $N = 0.5\text{--}0.7$ wt.%. It was shown that austenitic steel alloyed with nitrogen (N) has higher resistance to IDL in case of “soft” projectiles ($\approx 35\%$) and armor-piercing projectiles ($\approx 10\%$) compared to high-strength steel of medium hardness, the properties of which are similar to those of steel 20HGSNM [4, 5].

By analyzing the literature data related to the mechanical properties of high-strength nitrogen-alloyed austenitic steels [15–19], it became possible to establish an alloying system for metal-cored (powder) wire to solve the problems formulated above [2]. The main selected alloying elements were: C, Cr, Mn, Ni, Mo, Cu, and N.

Alloying with Cr results in strengthening of the solid solution and increased solubility of N in Fe. The typical chromium content of nitrogen-alloyed steels varies between 12.0 and 22.0 wt.% [18]. Further increase in Cr content above 23 wt.% leads to a sharp decrease in strength characteristics (ductility and toughness) [2, 17] due to the appearance of brittle σ -phase [19], while keeping the Cr content below 12.0 wt.% does not allow for a complete dissolution of N in Fe. To prevent the formation of the σ -phase, the Cr content is limited to 22.0–23.0 wt.%. In this case, the Mn content is increased to 4.0–6.0 wt.% to help maintain high solubility of N in steel and promote the formation of the austenitic structure.

In addition to $Mn = 4.0\text{--}6.0$ wt.%, the following amounts of nitrogen and nickel were introduced to obtain the austenitic structure: $N = 0.25\text{--}0.40$ wt.% and $Ni = 3.0\text{--}5.0$ wt.%. The excess of nitrogen ($N > 0.40$ wt.%) results in the appearance of pores in the weld metal, while at $N < 0.25$ wt.%, the austenitic structure cannot be formed. Nitrogen stabilizes the γ -phase, reduces the onset temperature of the martensitic transformation (M_{onset}), participates in various steel strengthening mechanisms (e.g., solid solution-, grain boundary-, and dispersion-based) [20–22], and enables the development of environmentally friendly materials by partially replacing Ni and Mn [15]. Alloying with nitrogen along with 3.0–5.0 wt.% Ni is more effective in terms of increasing the ultimate strength (σ_u) and yield strength ($\sigma_{0.2}$) of steels compared to nickel-free steels [19].

The introduction of Mo into the steel enhances resistance to pitting corrosion, strength level, impact toughness, and promotes the solubility of N in Fe. When the Mo content exceeds 3.5 wt.%, the steel becomes prone to aging, which causes precipitation of the χ -phase, negatively affecting the ductility and impact toughness (similar to the σ -phase). The optimal Mo content is between 2.0 and 3.0 wt.% [17].

Alloying stainless steels with up to 3.0 wt.% Cu enhances the corrosion resistance in hydrochloric and sulfuric acids and improves the stress corrosion endurance of H18N8 type steels with 0.5–2.0 wt.% Cu, which is associated with a significant increase in austenite stability even after a substantial cold working (steel remains non-magnetic) [23]. Copper tends to improve mechanical properties (especially, $\sigma_{0.2}$) during dispersion hardening as a result of ongoing aging processes (precipitation of the ϵ -phase). Combined alloying with Mo and Cu provides the most intensive strengthening of steel, which is associated with Cu precipitation [24]. It has been shown that the highest levels of strength and ductility are achieved as a result of combined alloying with Cu, Ni, and N [25]. However, excessive alloying with Cu (above 3.0 wt.%) reduces the steel resistance to cold temperatures.

Ti and Al increase the solubility of N in Fe, however, excessive alloying with these elements leads to the formation of nitrides (e.g., TiN, AlN + Al_2O_3). Titanium nitrides (TiN) have a tendency to coagulate, while forming extensive colonies, which reduce the steel toughness. The addition of Al leads to the formation of

Table 1
Welding Parameters

I_w , A	U_A , B	V_w , m/h	q/v , MJ/m
136	23.6	11.7	0.4145
129	24.0	12.5	0.3564
129	23.6	10.6	0.4062
130	23.8	7.9	0.5628
130	23.6	6.8	0.6449
Root pass			
143	23.4	7.8	0.6881
133	23.3	8.3	0.5427

Comments: I_w – welding current, A; U_A – arc voltage, V; V_w – welding speed, m/h; q/v – weld heat input, MJ/m.

stringer-type inclusions at the grain and twin boundaries, which results in a decrease in the ductile characteristics and toughness of steel [17].

Materials and Procedures

The deposited metal obtained by using the developed EMs (diameter – 1.6 mm) was studied. The deposition welding was performed in 12 passes (deposit height > 22 mm) using a 20 mm thick sheet of steel 3 (according to GOST 380). The welding parameters were as follows: welding current $I_w = 148$ A, arc voltage $U_A = 23$ V, welding speed $V_w = 6.0$ m/h.

The chemical composition of the developed material (Cr20Mn5Ni4Mo2.5Cu3N0.3) was as follows, wt.-%: C ≤ 0.15; Si ≤ 0.80; Mn = 4.0–6.0; Cr = 18.0–22.0; Ni = 3.0–5.0; Mo = 2.0–3.0; Cu = 2.0–3.5; and N = 0.25–0.40.

The welding was performed using plates measuring 150 × 300 × 18.9 mm, with weld groove geometry of C17 (GOST 14771). The plate material was high-strength alloy steel 20HGSNM, heat-treated to achieve high hardness (quenching from 900–950°C, holding for 1 hour, tempering at 270 ± 10°C for 4 hours, $HRC = 43–7$). The chemical composition of steel 20HGSNM is as follows: 0.18–0.24 C; 1.20–1.50 Si; 0.30–0.60 Mn; 1.10–1.40 Cr; 0.50–0.80 Ni; 0.15–0.25 Mo [5].

Arc welding and weld deposition were performed using the Lorch S5 SpeedPulse XT machine in the protective gas atmosphere CORGON 18 (82% Ar + 18% CO₂). Arc welding was performed in five passes with flux backing. On the back side of the weld, a weld root grinding was performed to produce a groove (width – 8 mm, depth – 4 mm), followed by stringer welding in two passes. The welding parameters are presented in Table 1.

The chemical analysis was performed using the Spectromaxx spectrometer, AN-7529 carbon express analyzer, and ON-900 oxygen and nitrogen analyzer. Static tensile testing of the deposited metal (DM) was performed on type II samples according to GOST 6996 using the Tinius Olsen H50KS tester (50 kN).

Table 2
Mechanical Characteristics of Deposited Metal

Wire	σ_u , MPa	$\sigma_{0.2}$, MPa	δ , %
Sv-10GSMT (GOST 2246–70)	640	450	24
Sv-08H20N9G7T (GOST 2246–70)	600	320	33
Cr20Mn5Ni4Mo2.5Cu3N0.3	820	570	42

The microhardness of the welded joint was measured using the KBW-1 microhardness tester (by KB Prüftechnik GmbH) under a load of 0.1 kg-f ($HV_{0.1}$) according to GOST 57180. Metallographic analysis was conducted using the Olympus GX53 optical microscope. X-ray spectral microanalysis was performed using the TESCAN VEGA II XMU scanning electron microscope with an integrated energy-dispersive INCA Energy 450XT attachment. Thermal and deformation stability were evaluated using the calculated temperature values M_{onset} [16, 26] and M_{D30} [16, 19, 27, 28]. The quantitative analysis of the structural components of the deposited metal (DM) and weld metal (WM) was conducted using the Image pro software. The presence of ferrite in the DM (δF) was determined using the MK-1F ferrite meter.

The deposited metal was analyzed for chemical elements using an electron microscope with wavelength-dispersive spectroscopy (WDS) EDAX TEAM.

Data Analysis

The results of chemical analysis of the deposited metal using the developed metal-cored wire (Cr20Mn5Ni4Mo2.5Cu3N0.3) were as follows, wt.%: 0.14 C; 0.40 Si; 5.0 Mn; 20.4 Cr; 3.70 Ni; 2.30 Mo; 3.20 Cu; and 0.30 N.

The deposited metal exhibits high toughness and no visible defects, such as pores, cracks, or slag inclusions. The developed compositions meet the requirements of the industry standard for the production of special equipment [29].

The values of σ_u and $\sigma_{0.2}$ of the composition Cr20Mn5Ni4Mo2.5Cu3N0.3 are 20 to 30% higher than those of the currently used EMs (Table 2), while the ductility is maintained at a relatively high level ($\delta = 43\%$).

The temperature values of $M_{onset} = -195^\circ\text{C}$ and $M_{D30} = -146.5^\circ\text{C}$ for the composition Cr20Mn5Ni4Mo2.5Cu3N0.3 indicate that the metal possesses a stable structure that is not prone to $\gamma \rightarrow \epsilon$ -transformations during deformation.

According to the results of X-ray spectral microanalysis (Fig. 1, 2), the metal structure contains the following elements: carbon, nitrogen, chromium, manganese, nickel, molybdenum, and copper. The deposited metal exhibits inclusions of molybdenum and chromium carbides at the grain boundaries due to their precipitation from the adjacent grain boundary regions. Nitrogen (Fig. 2b) is uniformly distributed within the bulk of the metal and practically does not accumulate at the grain boundaries.

The structure of the deposited metal Cr20Mn5Ni4Mo2.5Cu3N0.3 is austenite with δF (Fig. 3).

According to data obtained by using the ferrite meter, the quantitative content of δF in the deposited metal is 1.5 vol. %, which is consistent with the calculation results according to the Schaeffler diagram ($\delta F \approx 0.5$ vol. %) and image analysis using *Image Pro* software ($\delta F \approx 3.0$ vol. %).

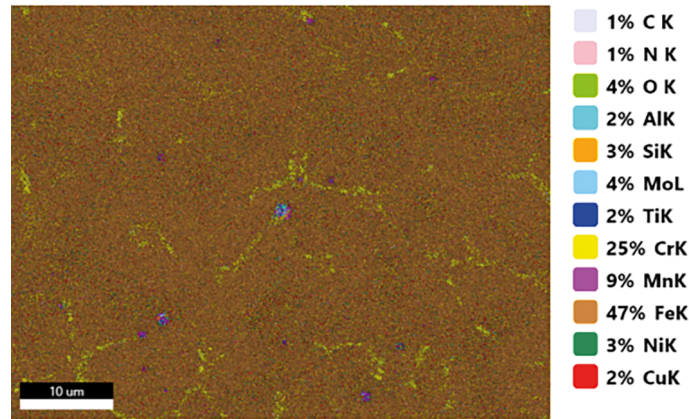


Fig. 1. Phase composition map (Cr20Mn5Ni4Mo2.5Cu3N0.3).

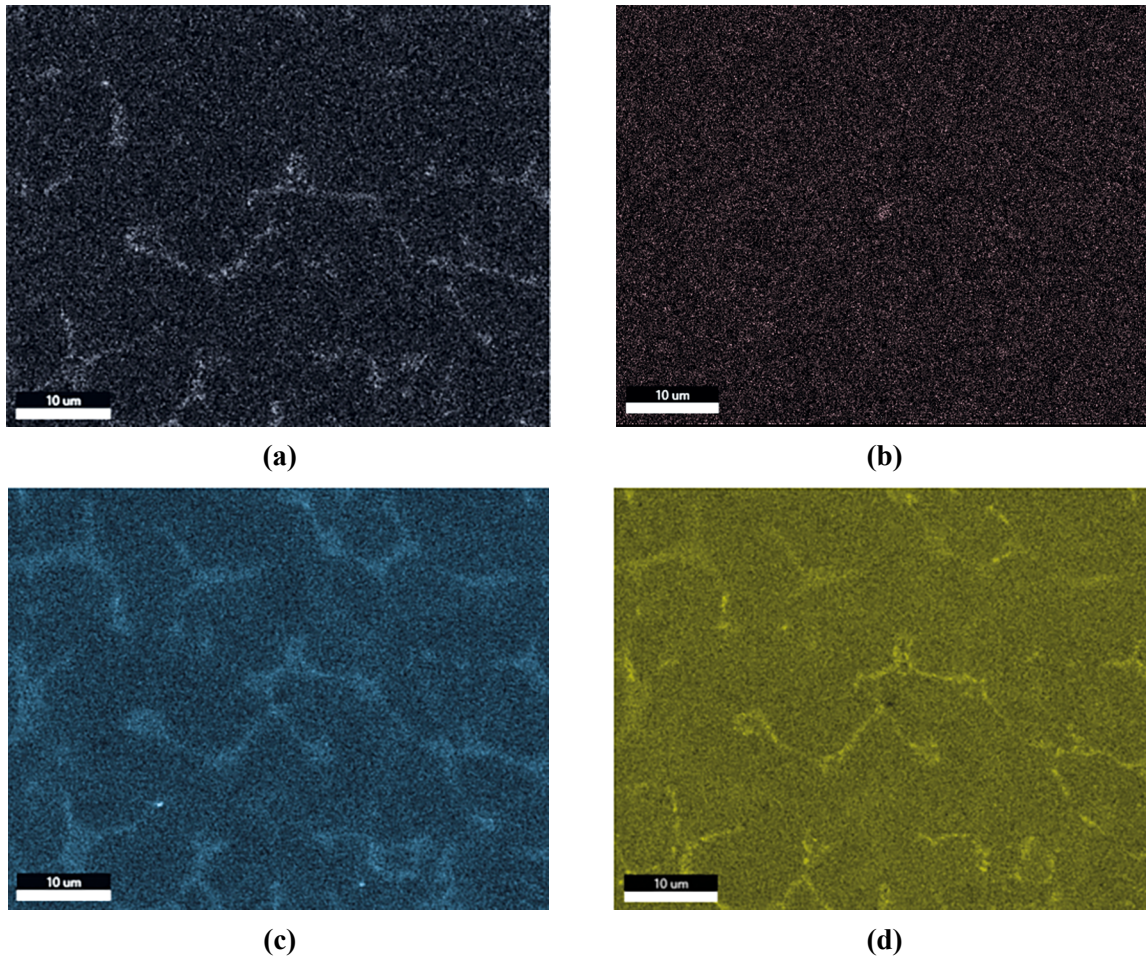


Fig. 2. Phase composition map (Cr20Mn5Ni4Mo2.5Cu3N0.3 alloy): (a) C K ROI; (b) N K ROI; (c) Mo K ROI; (d) Cr K ROI.

Results of the base metal chemical analysis (steel 20HGSNM) are as follows, wt.%: 0.225 C; 1.30 Si; 0.36 Mn; 1.30 Cr; 0.65 Ni; and 0.16 Mo [29]. The structure of steel 20HGSNM represents a mixture of lower bainite and an insignificant quantity of low-tempered lath martensite (Fig. 4).

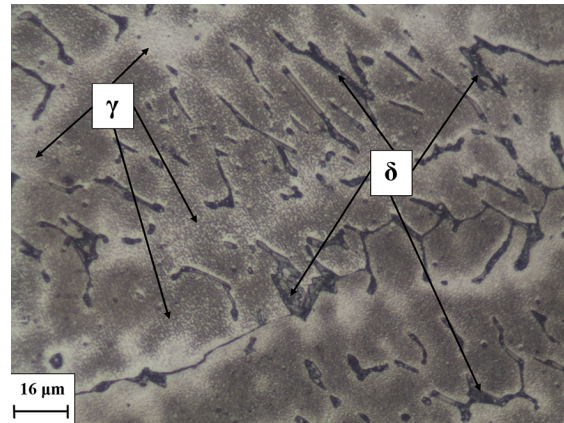
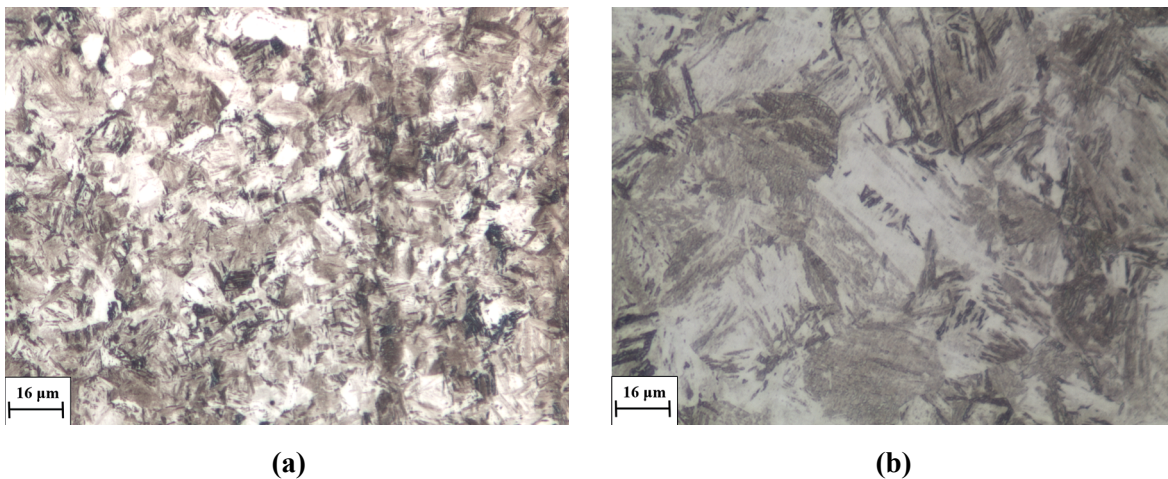


Fig. 3. Structure of the deposited metal (Cr20Mn5Ni4Mo2.5Cu3N0.3), $\times 400$.



(a)

(b)

Fig. 4. Structure of steel 20HGSNM: (a) $\times 100$; (b) $\times 400$.

After welding, no visible defects, such as pores, cracks, or slag inclusions were found in the welded joints. Only a small amount of spatter was observed. An austenitic-ferritic structure was formed in the weld metal (Fig. 5, 3). The resulting structure is consistent with data reported in other studies [30].

In the heat-affected zone (HAZ) near the weld metal (Fig. 6(1)), a $\gamma \rightarrow \alpha$ -transformation occurred, resulting in significant growth of austenite grains up to 50–500 μm in size. The structure consisted of pearlite and bainite with interlayers of austenite. At a distance of about 350 μm from the weld metal, the $\gamma \rightarrow \alpha$ -transformation resulted in the martensite formation in the form of plate packets (Fig. 6(2)). At a distance of 700 μm from the weld metal (Fig. 6(3)), the structure consists of martensite, bainite, and some amount of δF .

The results of static tensile testing of type XIIIa welded samples (according to GOST 6996) are as follows: $\sigma_u = 728 \text{ MPa} = 74.3 \text{ kg/mm}^2$. The strength of the welded joint produced using the developed metal-cored wire (Cr20Mn5Ni4Mo2.5Cu3N0.3) is 20% higher compared to welded joints produced with the solid wire (Sv-08X20N9G7T) (the strength of the welded joints does not exceed 600 MPa). The fracture of the sample occurred along the fusion zone [29]. The strength of the welded joint is 11.2% lower than the strength of the base material, which is associated with the structure in the heat-affected zone (HAZ). It is known that the performance of the entire structure is determined not so much by the base material, but by the mechanical characteristics of

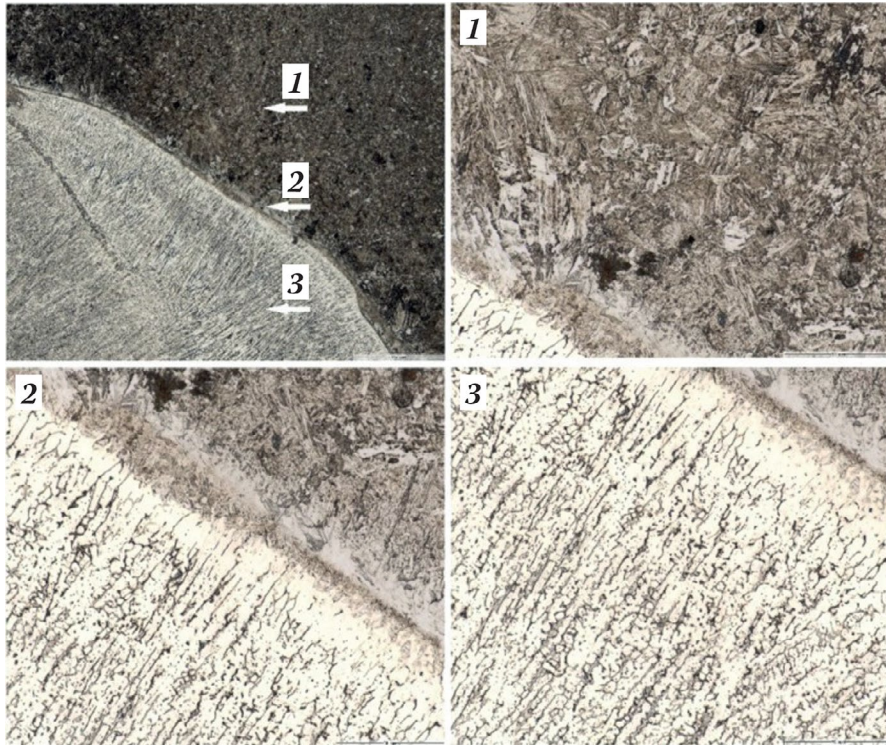


Fig. 5. Structure of the welded joint, $\times 100$: 1 – HAZ, $\times 400$; 2 – fusion zone, $\times 400$; 3 – weld metal, $\times 400$.

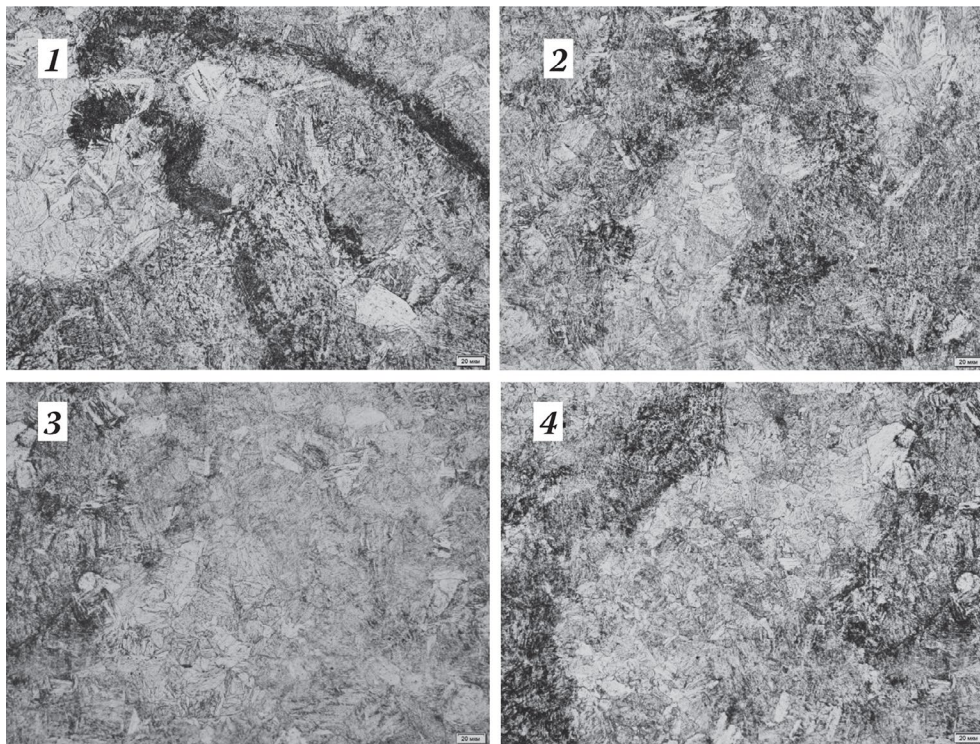


Fig. 6. HAZ structure, $\times 500$: 1 – hot spot; 2 – 350 μm away from the weld; 3 – 700 μm away from the weld; 4 – 1,000 μm away from the weld.

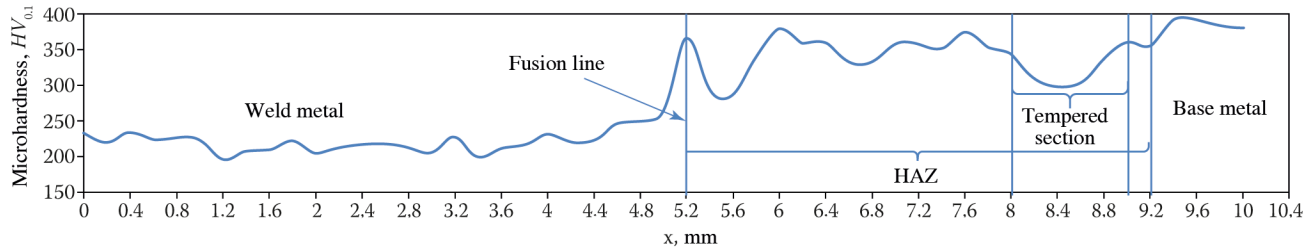


Fig. 7. Microhardness distribution.

the HAZ, which depend on the chemical, structural, and phase compositions, as well as the grain size [6]. Coarse grains in the heat-affected zone with decarburized boundaries around lath martensite formations (Fig. 6(1)) negatively affect the mechanical characteristics.

No sharp changes in the microhardness values were recorded when measuring microhardness of the welded joint according to GOST 57180.

The microhardness of the weld metal varies within a range of 200–250 $HV_{0.1}$, which is consistent with the resulting austenitic structure of the welded joint in this area as determined by metallographic analysis. The microhardness of the heat-affected zone, which is 3.5–4.0 mm long, ranges from 280 to 380 $HV_{0.1}$ (Fig. 7). The maximum microhardness along the fusion line constitutes 366 $HV_{0.1}$, which is consistent with the pearlite and bainite structure identified during the metallographic analysis. The length of the HAZ tempering zone, which was heated to 800–500°C, is about 1.0 mm. The structure and properties of the HAZ are controlled by changing the cooling rates in the near-weld zone, which can be achieved in most cases by adjusting the weld heat input (q/v , MJ/m). It is known that austenitic electrode materials have lower solidus temperatures (by 50–100°C) compared to ferrite-pearlite grade materials [2, 6, 7, 31]. This reduces the overheating of the near-weld zone due to a shorter metal residence time above the intensive grain growth temperature (A_{c3}). The absence of polymorphic transformation $\gamma \rightarrow \alpha$ in the weld metal and increased deformation capacity of the austenitic structure, along with significantly higher (by an order of magnitude) hydrogen solubility and lower diffusion coefficient, as well as a good combination of ductility and toughness substantially reduce the metal susceptibility to cracking. In this regard, the use of metal-cored wire allows for a “softer” thermal welding cycle compared to solid wires, which further reduces the overheating of the near-weld zone and improves the mechanical properties of this area.

By analyzing Ref. [6, 7, 32], it can be shown that the optimal structure in the near-weld zone during welding of high-strength alloy steels mainly consists of lower bainite with low-tempered lath martensite and has a hardness of 200–350 HV . Further studies will be dedicated to determining the optimal cooling rate in the HAZ during welding with the use of austenitic metal-cored wire to obtain the most favorable structure and properties in the near-weld zone along with minimized length of the heat-affected zone. Additional studies will be conducted to assess the impact of intense dynamic loads of metal object on the weld metal, and to analyze its structure and properties after the test.

CONCLUSIONS

An austenitic metal-cored wire Cr20Mn5Ni4Mo2.5Cu3N0.3 alloyed with nitrogen (N = 0.25–0.40 wt.%) has been developed for gas-shielded welding of high-strength alloy steels.

The structure of the deposited metal (Cr20Mn5Ni4Mo2.5Cu3N0.3) consists of austenite with 1.0–3.0 vol. % δF . The structure of the base metal (steel 20HGSNM) before welding consists of a mixture of lower

bainite and a small amount of low-tempered lath martensite. In the heat-affected zone (HAZ) near the weld, bainite, pearlite with austenite interlayers, and significant grain growth of up to 50–500 μm are observed. At a distance of about 0.7 mm from the fusion line, the base metal structure is represented by martensite, bainite, and some amount of δF . The total HAZ length is 3.5–4.0 mm.

The HAZ microhardness varies within the range of 280–380 $HV_{0.1}$ and reaches 366 $HV_{0.1}$ along the fusion line. The microhardness of the weld metal ranges from 200 to 250 $HV_{0.1}$.

The strength of the welded joint made with Cr20Mn5Ni4Mo2.5Cu3N0.3 wire is 728 MPa, which is about 20% higher compared to the currently used Sv-08H20N9G7T type wires (up to 600 MPa).

This research was sponsored by the Innovation Promotion Fund under the “Umnik” program (Agreement No. 17779GU/2022 dated May 13, 2022).

REFERENCES

1. T. A. Rakhmatullin, M. A. Sholokhov, and D. S. Buzorina, “Problems of implementing tapered grooves during welding of hull structures of special equipment,” *Izv. Vuzov*, No. 4, 64–66 (2012).
2. M. P. Shalimov, A. V. Berezovsky, and A. S. Smolentsev, “Development of technology and powder wire for arc welding of high-strength alloyed steels,” *Vestn. PNIPU, Mashinostroyeniye, Materialovedeniye*, **21**, No. 1, 49–54 (2019).
3. S. A. Gladyshev and V. A. Grigoryan, *Armored Steels* [in Russian], Internet Engineering, Moscow (2010).
4. M. A. Sholokhov, S. A. Kurkin, and S. I. Poloskov, “Evaluation of the effect of groove shape and welding modes on residual stresses in structural components of special equipment,” *Svarka i Diagnostika*, No. 6, 50–55 (2014).
5. T. I. Tabatchikova, N. A. Tereshchenko, A. N. Morozova, and N. Z. Gudnev, “Effect of intensive dynamic impact on phase and structural transformations in the metal of welded joints,” *Fizika Metallov i Metallovedeniye (FMM)*, **120**, No. 6, 661–667 (2019).
6. A. V. Berezovsky, A. S. Smolentsev, M. P. Shalimov, M. S. Smolentsev, and A. N. Balin, “Current state and challenges of weldability of high-strength quench-hardening steels,” *Tyazheloe Mashinostroyeniye*, No. 7-8, 2–9 (2021).
7. A. S. Smolentsev, “Ways to solve the weldability problems of high-strength steels prone to hardening (review),” *Svarka i Diagnostika*, No. 3, 48–53 (2019).
8. A. S. Smolentsev, “New material for arc welding of high-strength medium-alloyed steels,” in: *Welding, Renovation, Triboengineering: Materials of the 9th Ural Scientific and Practical Conference* [in Russian], Nizhny Tagil: NTI (branch) of UrFU (2019), pp. 70–75.
9. N. P. Borovinskaya, V. I. Shumyakov, and G. S. Vasiliev, “New materials for welding armor,” *Vest. Bronetank. Tekhn.*, No. 5, 45–47 (1977).
10. G. Magudeeswaran, V. Balasubramanian, and G. Madhusudan Reddy, “Metallurgical characteristics of armour steel welded joints used for combat vehicle construction,” *Defence Technology*, No. 14, 590–606 (2018).
11. V. P. Korobko, P. B. Smirnov, N. Z. Gudnev, Yu. S. Korobov, V. I. Shumyakov, V. G. Shipsha, V. A. Bychenok, D. S. Ashikhin, V. Ye. Prokhorovich, I. Ye. Alifanova, I. A. Bepalov, A. V. Ilyin, P. V. Melnikov, A. N. Balin, and M. A. Sholokhov, “Brief description of the technology for obtaining new welding materials and welding technologies based on them for the manufacture of light-armored vehicles with bulletproof welded joints at the base metal level for steels: St7, A3, and 44SVSh,” in: *Relevant Problems of Protection and Safety: Proc. of the 22nd All-Russian Scientific and Practical Conference RARAN (April 1-4, 2019)*, Federal State Budgetary Institution “Russian Academy of Rocket and Artillery Sciences,” St. Petersburg (2019), pp. 127–136.
12. S. Ye. Aleksentseva, *Impact-Wave Processes of High-Speed Elements Interaction with Condensed Media* [in Russian], Abstract of the Dissertation (Doctor of Technical Sciences), Samara (2015).
13. R. Mohammed, M. Reddy, and K. Srinivasa Rao, “Welding of nickel free high nitrogen stainless steel: Microstructure and mechanical properties,” *Defence Technology*, **13**, No. 2, 59–71 (2017).
14. B. Singh, G. P. Sukumar, S. Ponguru, P. Jena, R. Pochana, K. Kumar, V. Madhu, and G. Reddy, “Future armour materials and technologies for combat platforms,” *Defence Sci. J.*, **67**, 412 (2017).
15. V. V. Sagadze and A. I. Uvarov, *Strengthening and Properties of Austenitic Steels* [in Russian], RIO URO RAN, Yekaterinburg (2013).
16. L. M. Kaputkina, I. V. Smarigina, A. G. Svyazhin, V. E. Kindop, and Ye. V. Blinov, “Structural stability and properties of nitrogen-containing high-strength austenitic steels under cyclic thermal and mechanical loads,” *MiTOM*, No. 1 (763), 3–9 (2019).
17. I. V. Gorynin, V. A. Malyshevskii, G. Yu. Kalinin, S. Yu. Mushnikova, O. A. Bannykh, V. M. Blinov, and M. V. Kostina, “Corrosion-resistant high-strength nitrogen-containing steels,” *Voprosy Materialovedeniya, Central Research Institute of Structural Materials “Prometei,” St. Petersburg*, No. 3 (59), 7–16 (2009).

18. I. O. Bannykh, “Structural specifics and application prospects of high-nitrogen austenitic steels,” *MiTOM*, No. 5 (767), 22–29 (2019).
19. V. V. Berezovskaya and A. V. Berezovsky, *Corrosion-Resistant Steels and Alloys* [in Russian], Publ. Ural. Univ., Yekaterinburg (2019).
20. A. G. Svyazhin and L. M. Kaputkina, “Nitrogen and high-nitrogen steels: industrial technologies and properties,” *Izv. Vuzov. Chernaya Metallurgiya*, **62**, No. 3, 173–187 (2019).
21. M. V. Kostina and L. G. Rigina, “Nitrogen-containing steels and methods of their production,” *Izv. Vuzov. Chernaya Metallurgiya*, **63**, No. 8, 606–622 (2020).
22. Ts. V. Rashev, A. V. Yeliseev, L. T. Zhekova, and P. V. Bogevev, “High-nitrogen steels,” *Izv. Vuzov. Chernaya Metallurgiya*, **62**, No. 7, 503–510 (2019).
23. E. Goodremon, *Special Steels* [in Russian], in 2 vol., Vol. 2, transl. from German, ed. by A. S. Zaimovskii, corr. member of the USSR Academy of Sciences, Metallurgiya, Moscow (1966).
24. *Copper in Ferrous Metals* [in Russian], ed. by I. Le Mei and L. M.-D. Shetki, transl. from English by I. D. Marchukova and A. N. Shteynberg, ed. by O. A. Bannykh, Metallurgiya, Moscow (1988).
25. M. V. Pridantsev, N. P. Talov, and F. L. Levin, *High-strength Austenitic Steels* [in Russian], Metallurgiya, Moscow (1969).
26. S. R. Birman, *Economically Alloyed Martensite-aging Steels* [in Russian], Metallurgiya, Moscow (1974).
27. F. B. Pickering, *Physical Metallurgy and the Design of Steels* [in Russian], Metallurgiya, Moscow (1982).
28. F. B. Pickering, *Physical Metallurgy and the Design of Steels*, Applied Science Publisher Ltd, London (1978).
29. A. S. Smolentsev, “Strength characteristics of deposited metal and welded joints made with TWIP-austenitic powder wire,” in: *21st Int. Sci. Techn. Ural School-Seminar of Young Metallurgy Scientists* [in Russian], Ural Federal University, Yekaterinburg (2022), pp. 400–405.
30. D. Lippold, *Welding Metallurgy and Weldability of Stainless Steels* [in Russian], transl. from English by N. A. Sosnin and A. M. Levchenko, Polytechn. Univ. Publ., St. Petersburg (2011).
31. T. I. Tabatchikova, A. D. Nosov, S. N. Goncharov, N. Z. Gudnev, S. Yu. Delgado Reina, and I. L. Yakovleva, “Structure and viscosity of the heat-affected zone of welded joints of high-strength steel,” *Fizika Metallov i Metallovedenie*, **115**, No. 12, 1309–1317 (2014).
32. E. L. Makarov and B. F. Yakushin, *Theory of Weldability of Steels and Alloys* [in Russian], Bauman Moscow State Technical University Publ., Moscow (2014).